

PAPER

Evidence for negative thermal expansion in the superconducting precursor phase SmFeAsO

To cite this article: H D Zhou *et al* 2018 *J. Phys.: Condens. Matter* **30** 095601

View the [article online](#) for updates and enhancements.

Related content

- [Absence of superconductivity in fluorine-doped neptunium pnictide NpFeAsO](#)
A C Walters, H C Walker, R Springell *et al.*
- [Transport and infrared properties of SmFeAs\(O_{1-x}F_x\): from SDW to superconducting ordering](#)
M Tropeano, C Fanciulli, C Ferdeghini *et al.*
- [An overview on iron based superconductors](#)
P M Aswathy, J B Anooja, P M Sarun *et al.*



Instruments for Advanced Science

Contact Hiden Analytical for further details:
W www.HidenAnalytical.com
E info@hiden.co.uk

CLICK TO VIEW our product catalogue



Gas Analysis

- dynamic measurement of reaction gas streams
- catalysis and thermal analysis
- molecular beam studies
- dissolved species probes
- fermentation, environmental and ecological studies



Surface Science

- UHV-TPD
- SIMS
- end point detection in ion beam etch
- elemental imaging - surface mapping



Plasma Diagnostics

- plasma source characterization
- etch and deposition process reaction kinetic studies
- analysis of neutral and radical species



Vacuum Analysis

- partial pressure measurement and control of process gases
- reactive sputter process control
- vacuum diagnostics
- vacuum coating process monitoring

Evidence for negative thermal expansion in the superconducting precursor phase SmFeAsO

H D Zhou¹, P M Sarte^{2,3}, B S Conner⁴, L Balicas⁵, C R Wiebe^{6,7,8,9,14}, X H Chen^{10,11,12}, T Wu^{10,11,12}, G Wu¹⁰, R H Liu¹³, H Chen¹⁰ and D F Fang¹⁰

¹ Department of Physics and Astronomy, University of Tennessee, Knoxville, TN 37996, United States of America

² School of Chemistry, University of Edinburgh, Edinburgh, EH9 3FJ, United Kingdom

³ Centre for Science at Extreme Conditions, University of Edinburgh, Edinburgh, EH9 3FD, United Kingdom

⁴ Materials Science and Technology Division, Oak Ridge National Laboratory, Oak Ridge, TN 37831, United States of America

⁵ National High Magnetic Field Laboratory, Florida State University, Tallahassee, FL 32306-4005, United States of America

⁶ Department of Chemistry, University of Winnipeg, Winnipeg, MB R3B 2E9, Canada

⁷ Department of Physics and Astronomy, McMaster University, Hamilton, ON L8S 4M1, Canada

⁸ Canadian Institute for Advanced Research, Toronto, ON M5G 1Z8, Canada

⁹ Department of Chemistry, University of Manitoba, Winnipeg, MB R3T 2N2, Canada

¹⁰ Hefei National Laboratory for Physical Sciences at Microscale and Department of Physics, University of Science and Technology of China, Hefei, Anhui 230026, People's Republic of China

¹¹ Collaborative Innovation Center of Advanced Microstructures, Nanjing University, Nanjing 210093, People's Republic of China

¹² Key Laboratory of Strongly-coupled Quantum Matter Physics, University of Science and Technology of China, Chinese Academy of Sciences, Hefei 230026, People's Republic of China

¹³ Department of Physics, Emory University, Atlanta, GA 30322, United States of America

E-mail: ch.wiebe@uwinnipeg.ca

Received 21 September 2017, revised 16 December 2017

Accepted for publication 22 December 2017

Published 12 February 2018



Abstract

The fluorine-doped rare-earth iron oxypnictide series SmFeAsO_{1-x}F_x ($0 \leq x \leq 0.10$) was investigated with high resolution powder x-ray scattering. In agreement with previous studies (Margaritona *et al* 2009 *Phys. Rev. B* **79** 014503), the parent compound SmFeAsO exhibits a tetragonal-to-orthorhombic structural distortion at $T_S = 130$ K which is rapidly suppressed by $x \simeq 0.10$ deep within the superconducting dome. The change in unit cell symmetry is followed by a previously unreported magnetoelastic distortion at 120 K. The temperature dependence of the thermal expansion coefficient α_V reveals a rich phase diagram for SmFeAsO: (i) a global minimum at 125 K corresponds to the opening of a spin-density wave instability as measured by pump-probe femtosecond spectroscopy (Mertelj *et al* 2010 *Phys. Rev. B* **81** 224504) whilst (ii) a global maximum at 110 K corresponds to magnetic ordering of the Sm and Fe sublattices as measured by magnetic x-ray scattering (Nandi *et al* 2011 *Phys. Rev. B* **84** 055419). At much lower temperatures than T_N , SmFeAsO exhibits a significant negative thermal expansion on the order of -40 ppm \cdot K⁻¹ in contrast to the behaviour of other rare-earth oxypnictides such as PrFeAsO (Kimber *et al* 2008 *Phys. Rev. B* **78** 140503) and the actinide oxypnictide NpFeAsO (Klimczuk *et al* 2012 *Phys. Rev. B* **85** 174506) where the onset of $\alpha_V < 0$ only appears in the vicinity of magnetic ordering. Correlating this feature with the temperature and doping dependence of the resistivity and the unit cell parameters, we interpret the negative thermal expansion as being indicative of the possible

¹⁴ Author to whom any correspondence should be addressed.

condensation of itinerant electrons accompanying the opening of a SDW gap, consistent with transport measurements (Tropeano *et al* 2009 *Supercond. Sci. Technol.* **22** 034004).

Keywords: x-ray diffraction, superconductivity, negative thermal expansion, magnetism, low temperature property measurements, strongly correlated electron systems

(Some figures may appear in colour only in the online journal)

The discovery of iron oxypnictides of the general formula $RFeAsO$ ($R = RE^{3+}$) has brought about a renaissance in the field of high temperature superconductivity [1–3]. Previous efforts were almost completely focused on the cuprates for nearly two decades, with no real clear picture emerging for the superconducting mechanism or an explanation of the rich phase diagrams as a function of doping [4–15]. It has been well-understood that strong spin–spin coupling, in addition to the two-dimensional layers of square planar CuO plaquettes, and mobility introduced through electron and/or hole doping of the Mott insulator phases are common properties to all of the superconducting phases [16]. However, the discovery of superconductivity in the two-dimensional iron oxypnictide structures (with the $d^7 Fe^{2+}$) has left an indelible mark on the condensed matter community [17, 18]. A combination of the relatively high values of T_c [1, 19–27] for the earliest samples and the striking similarities of their rich phase diagrams to those of the cuprates [22–25, 26, 27–31] suggests that through further refinements of the chemistry, and an understanding of the mechanism, these iron oxypnictides and iron-based two-dimensional structures in general not only provide a potential route for advancing our understanding of the cuprates but may even provide T_c values challenging the records of the cuprates.

In this paper, we focus on x-ray studies of the fluorine-doped oxypnictide series $SmFeAsO_{1-x}F_x$ —a series with one of the highest T_c values (~ 58 K for optimal $x = 0.20$ [19]) among the iron-based superconductors. A prominent tetragonal-to-orthorhombic structural distortion is observed at $T_S = 130$ K in the parent compound $SmFeAsO$ corresponding to a peak in $\frac{d\rho}{dT}$, quickly followed by a previously unreported magnetoelastic coupling at $T^* = 120$ K. The temperature dependence of the thermal expansion coefficient α_V reveals that the transition at 120 K lies between a global minimum of the thermal expansion corresponding to the opening of a spin-density wave (SDW) instability as measured by pump-probe femtosecond spectroscopy [32] and a global maximum corresponding to magnetic ordering on both the Sm and Fe magnetic sublattices as measured by magnetic x-ray scattering [33]. Upon cooling to temperatures much below T^* , $SmFeAsO$ exhibits a significant negative thermal expansion, corresponding to a broad feature in $\frac{d\rho}{dT}$. Although previously unreported for $SmFeAsO$, this behaviour is reminiscent of other iron oxypnictides such as $PrFeAsO$ [37] and $LaFeAsO$ [38]. Since this behaviour has also been previously reported for $LaFeAsO$ [38] with a non-magnetic RE^{3+} site, the negative thermal expansion was interpreted as an effect due to electron localisation, specifically upon the Fe site, a claim that was also alluded to by systematic transport measurements on $SmFeAsO_{1-x}F_x$ [39]. Our interpretation of the data is supported

by the observed suppression of all anomalous features in the temperature dependence of the crystallographic parameters with minimal fluorine doping since it is well-documented that electron-doping across the $RFeAsO_{1-x}F_x$ ($R = RE^{3+}$) series induces superconductivity—by $x \sim 0.07$ [3, 40] for Sm—and the onset of superconductivity quickly suppresses the tetragonal-to-orthorhombic distortion, the SDW phase and the Néel phase [1, 26, 41–43]. Although the negative thermal expansion is quickly suppressed with minimal fluorine doping, it is worthwhile to note that since the lowest temperature anomaly occurs at an energy scale close to T_c in optimally doped samples [19–21], the negative thermal expansion may correspond to a SDW that is rapidly suppressed in the $SmFeAsO_{1-x}F_x$ series as superconductivity evolves.

Polycrystalline samples of $SmFeAsO_{1-x}F_x$ ($x = 0, 0.05$ and 0.10) were prepared by a two-step solid state reaction as previously outlined by Tropeano *et al* [39]. The precursor $SmAs$ was obtained by reacting high purity Sm and As metal at 600 °C for 3 h, and then at 900 °C for 5 h. A mixture of $SmAs$, Fe, Fe_2O_3 , and FeF_2 powders with the appropriate nominal stoichiometric ratio was then ground thoroughly and pressed into small pellets. These pellets were wrapped in Ta foil and sealed in an evacuated quartz tube and annealed at 1200 °C for 24 h. The pellets were then retrieved, reground, repressed and annealed at 1300 °C for a further 72 h. Resistivity measurements were performed by the conventional four-point-probe method using a Quantum Design PPMS. The powder x-ray diffraction (pXRD) patterns were recorded by a HUBER imaging plate Guinier camera 670 with monochromatised $Cu K_{\alpha,1}$ radiation. Polycrystalline samples of $SmFeAsO_{1-x}F_x$ were cooled to a base temperature of 10 K with a closed cycle cryostat and held at base temperature for 12 h, whilst after each temperature change, the samples were held at the desired temperature for 10 min with the objective of achieving thermal equilibrium and avoiding spurious features such as phase trapping.

Figure 1 shows the Rietveld refinement of the parent compound $SmAsFeO$ ($x = 0$). The pXRD data was fit using the FULLPROF/WINPLOTR suite [44, 45]. As summarised by table 1, the refined lattice parameters and atomic positions correlate well with previous structural studies confirming that $SmFeAsO$ adopts the layered $ZrCuSiAs$ -type structure corresponding to the tetragonal $P4/nmm$ space group [41, 46, 47]. A prominent structural distortion at $T_S = 130$ K was deduced by the observation of splitting of structural Bragg peaks. One such example includes the splitting of the (212) to the (312) and (132) as illustrated in figure 2, corresponding to a structural transition from the tetragonal $P4/nmm$ to orthorhombic $Cmma$, once again in agreement with previous synchrotron and physical property results [39–41, 46, 48]. As summarised

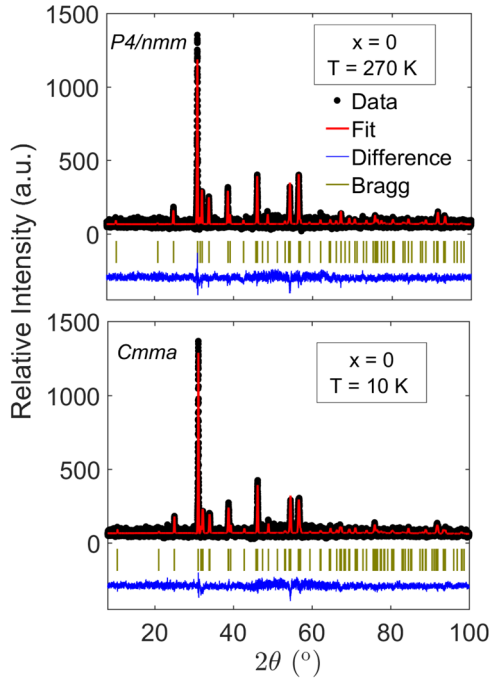


Figure 1. Measured, calculated and difference high resolution laboratory powder x-ray powder diffraction profiles for SmFeAsO at 270 K (tetragonal) and 10 K (orthorhombic) measured on a HUBER imaging plate Guinier camera 670 with Cu $K_{\alpha,1}$ radiation. The Bragg reflections' locations of the tetragonal $P4/nmm$ (270 K) and orthorhombic $Cmma$ (10 K) phases are given by the olive vertical lines.

Table 1. Refined crystallographic parameters at 270 K for SmAsFeO from the Rietveld refinement^a of the high resolution laboratory x-ray powder-diffraction profile. Numbers in parentheses indicate statistical errors.

Atom	Wyckoff site	x	y	z	B_{iso} (\AA^2)
Sm	$2c$	0.25	0.25	0.1364(3)	1.13(4)
Fe	$2b$	0.75	0.25	0.5	1.57(7)
As	$2c$	0.25	0.25	0.6632(5)	1.20(3)
O	$2a$	0.75	0.25	0	1.90(5)

^a Space group, $P4/nmm$. At 270 K, $a = 3.9402(2)$ \AA , $c = 8.4803(4)$ \AA , $V = 263.56(6)$ \AA^3 , $R_p \approx 6.0\%$, $R_{wp} \approx 6.0\%$ and $\chi^2 \approx 3.01$.

in figure 3(d), the resistivity of the parent compound shows a broad anomaly at higher temperatures but below this anomaly, there are no obvious features or phase transitions, consistent with previous transport measurements [3, 39, 49]. By taking the derivative of the resistivity, we find that there is a clear maximum at 130 K corresponding to the tetragonal-to-orthorhombic distortion temperature T_S . As shown in figure 4, the tetragonal-to-orthorhombic structural transition is quickly suppressed within the superconducting phase, in agreement with previous synchrotron results that deduced the complete suppression of the structural distortion by $x \sim 0.14$ [41]. Although the structural transition for $x = 0.05$ was detected through both the broadening of the (212) Bragg peak and a minor kink in the temperature evolution of a at 80 K which is well correlated with a peak in $\frac{d\rho}{dT}$ as illustrated in figures 4(a),(c) and (d), there is no such indication for the highest doped

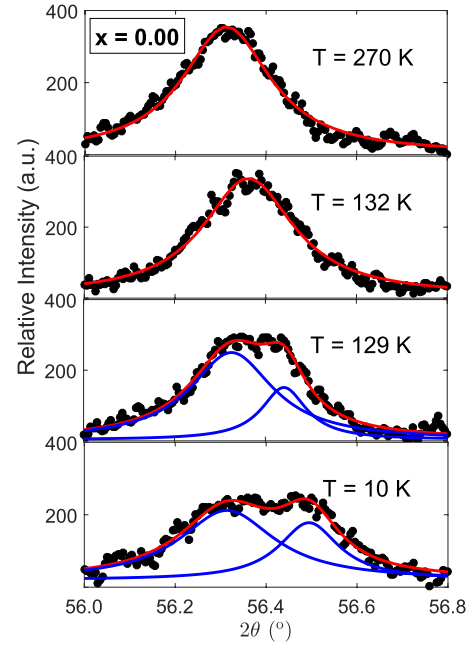


Figure 2. Temperature dependence of the (212) Bragg peak in the parent compound SmAsFeO ($x = 0$). The tetragonal-to-orthorhombic structural distortion at $T_S = 130$ K corresponds to the splitting of the (212) peak in the high temperature tetragonal $P4/nmm$ to the (132) and (312) peaks in the low temperature orthorhombic $Cmma$ phase. Solid red curves are the sum of fits to (132) and (312) individual peaks (solid blue curves) for the $Cmma$ phase or the (212) peak in the high temperature $P4/nmm$ phase.

sample ($x = 0.10$) due to the coarser resolution of the laboratory x-ray diffractometer used in this current study compared to ID31 at the ESRF utilised in previous studies [41].

From Rietveld refinements, the temperature evolution of the lattice parameters was calculated for the parent phase and are presented in figures 3(a)–(c) below. The first-order nature of the jump in both a and b is clear, in contrast with a more smooth evolution of c . Below T_S , a significant structural distortion was observed at 120 K. This previously unreported distortion manifests itself as a decrease of a , b , and c , and therefore a cusp-like feature of the unit cell volume V . A likely candidate for the 120 K transition is magnetic ordering accompanying a spin-density wave instability of the nested Fermi surface that is reminiscent of other rare-earth iron oxypnictides [1, 30, 43, 50]. Such a claim is supported by numerous observations in literature including the detection of spin-density wave ordering by pump-probe femtosecond spectroscopy at $T_{\text{SDW}} \simeq 125$ K [32] and the detection of long-range ordering of the Sm and Fe magnetic sublattices by magnetic x-ray scattering at $T_N \simeq 110$ K [33]. The formation of a SDW state below T_S is further supported by broad features in both DC susceptometry and heat capacity reported in literature [33, 51]. It is worthwhile to note that there exists a slight increase in the resistivity of the parent compound (figure 3) as one decreases temperature before both T_S and T_{SDW} in agreement with previous transport measurements [3, 39, 49]. This behaviour of the resistivity may correspond to the onset of magnetic correlations, reminiscent of the ‘stripe’ phase of $\text{La}_{1.6-x}\text{Nd}_{0.4}\text{Sr}_x\text{CuO}_4$ [52]. Furthermore, multiple

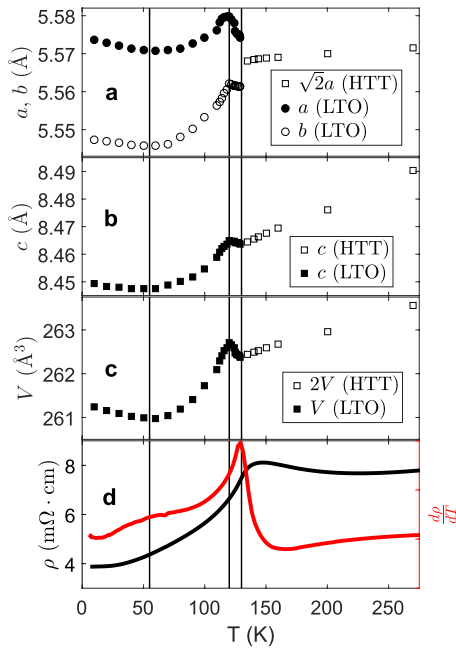


Figure 3. Temperature dependence of the a , b , and c lattice parameters for SmAsFeO (panels (a) and (b)) revealing a first order transition accompanying the tetragonal-to-orthorhombic distortion noted in figure 2. A strong magnetoelastic response at 120 K attributed to magnetic ordering ($T_N = 110$ K) following the opening of the SDW phase ($T_{SDW} = 125$ K) and is followed by a prominent negative thermal expansion in all three crystallographic phases beneath 55 K, far from the vicinity of any magnetic ordering. (c) The temperature dependence of the unit cell volume, exhibiting an anomaly at 120 K, followed by negative thermal expansion beneath 55 K. (d) The temperature dependence of the resistivity, and its derivative $\frac{d\rho}{dT}$. Note that a peak in $\frac{d\rho}{dT}$ occurs at 130 K and a broad anomaly appears as well at 55 K, coinciding with the onset of the tetragonal-to-orthorhombic distortion and the onset of negative thermal expansion, respectively. The labels HTT and LTO denote high temperature tetragonal phase and low temperature orthorhombic phase, respectively. N.B. Error bars are smaller than the size of the symbol representation of the experimental data.

studies [37, 53, 54] have correlated a broad feature in the resistivity at high temperatures preceding T_S with the formation of SDW phase. As illustrated in figure 4(d), this increase in the resistivity is quickly suppressed with fluorine doping $x \simeq 0.10$, corresponding to the onset of superconductivity in SmFeAsO $_{1-x}$ F $_x$ ($x \sim 0.07$ [3, 40]) and as is the case for other high temperature superconductors, the concurrent destruction of the SDW state and its accompanying magnetic ordering transition [3, 17]. The interpretation of the 120 K feature as magnetic ordering is strongly supported by the temperature dependence of the thermal expansion coefficient $\alpha_V = \frac{1}{V} \frac{\partial V}{\partial T}$ as presented in figure 5 below. The temperature dependence of α_V reveals a rich phase diagram where a global minimum and maximum corresponds to the aforementioned literature reported values of T_{SDW} [32] and T_N [33], respectively; whilst, the magnetoelastic transition at 120 K corresponds to the crossover between negative and positive thermal expansion, indicating that the 120 K transition corresponds to some exotic phase of SDW and Néel phase coexistence, both phases that ultimately compete [1, 34–36, 55] with superconductivity

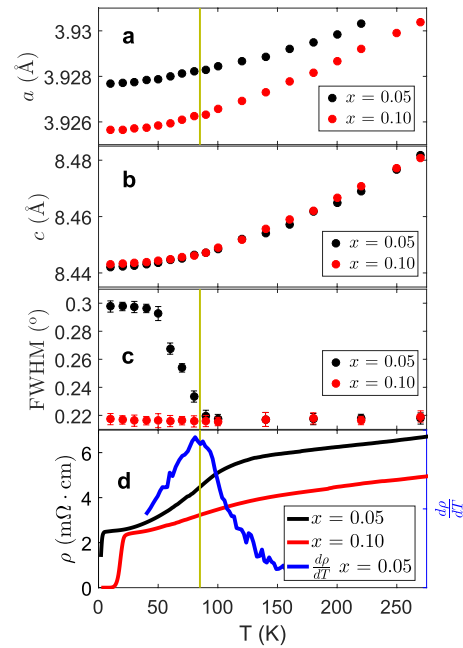


Figure 4. Comparison of the temperature dependence of the (a) a and (b) c lattice parameters for fluorine-doped members of the iron oxypnictide series SmFeAsO $_{1-x}$ F $_x$ ($x = 0.05, 0.1$). All anomalous features in figure 3 appear to have been completely suppressed with fluorine doping, consistent with the onset of superconductivity [1]. (c) Temperature dependence of the FWHM of the (212) peak identified a distinct broadening for $x = 0.05$, indicating the tetragonal-to-orthorhombic distortion persists in the presence of a small amount of fluorine doping, supported by the observation of a small kink in the temperature dependence of a in panel (a), consistent with previous synchrotron results [41]. The distortion appears to be completely suppressed by $x = 0.10$. (d) Temperature dependence of resistivity reveals that the high temperature upturn is substantially suppressed by $x = 0.05$ and completely suppressed by $x = 0.10$. A distinct peak in $\frac{d\rho}{dT}$ is well-correlated with both the onset of the broadening of the (212) peak and the kink in the temperature dependence of a for the $x = 0.05$ sample indicated by olive vertical lines.

and would be expected—and as is observed—to be quickly suppressed with fluorine doping.

As shown in figures 3 and 5, as SmFeAsO is cooled much below T_{SDW} , another anomalous feature appears at $T \approx 55$ K—a negative, nearly isotropic thermal expansion exists in all three crystallographic directions. The presence of a negative thermal expansion for SmFeAsO, although not been previously reported in either high resolution synchrotron [41] or three terminal capacitance measurements [56], has been detected in other rare-earth [37] and actinide oxypnictides [57]. The distinguishing feature of SmFeAsO is that the onset of negative thermal expansion does not coincide with any particular magnetic ordering process such as in NpFeAsO where the onset of $\alpha_V < 0$ coincides with T_N [57]. To gain some insight on the microscopic origin of the negative thermal expansion, we shall compare this system to other known materials that show negative thermal expansion. For a recent review on negative thermal expansion, please refer to Chen *et al* [58]. One obvious quantitative parameter for comparison is the coefficient thermal expansion $\alpha_V = -40$ ppm \cdot K $^{-1}$ at 10 K for the undoped

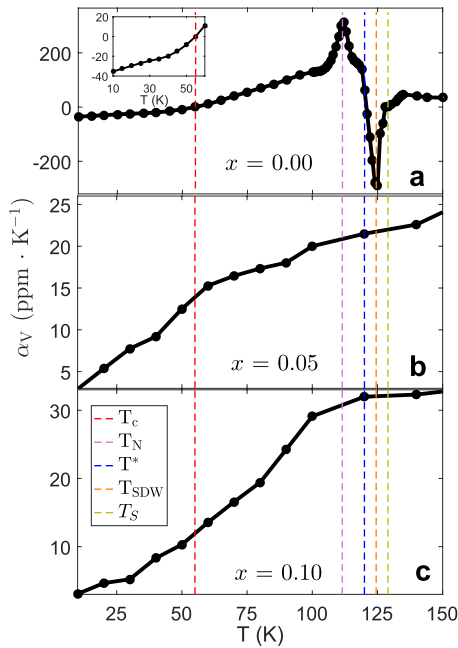


Figure 5. Temperature dependence of the thermal expansion coefficient α_V for (a) $x = 0.00$, (b) $x = 0.05$ and (c) $x = 0.10$ members of the fluorine-doped iron oxypnictide series $\text{SmFeAsO}_{1-x}\text{F}_x$. For the parent compound $x = 0$, the global maximum at 110 K and global minimum at 125 K correspond to magnetic ordering on the Sm and Fe magnetic sublattices as determined by magnetic x-ray scattering [33] and onset of the SDW phase as determined by pump-probe femtosecond spectroscopy [32], respectively. The three temperatures at which the value of α_V changes sign corresponds to the tetragonal-to-orthorhombic distortion temperature T_S , the magneto-elastic distortion temperature T^* and the critical temperature for optimally doped samples T_C [19–21]. As illustrated in the inset of (a), the parent compound exhibits a significant negative thermal expansion α_V of $-40 \text{ ppm} \cdot \text{K}^{-1}$ below T_C . The concurrent suppression of the negative thermal expansion at low temperatures and the anomalous features associated with the opening of the SDW gap with fluorine doping as illustrated in (b) and (c) strongly supports the interpretation of the negative thermal expansion as electron condensation due to the opening of the SDW gap as proposed by Tropeano *et al* [39].

compound. Simple fluorite structures with tetrahedrally coordinated atoms experience small negative thermal expansion with $\alpha_V \gtrsim -10 \text{ ppm} \cdot \text{K}^{-1}$ [59–63]. The tilting of rigid polyhedra in oxides with $O-M-O$ bridging in materials such as ZrW_2O_8 , heralded as a compound with significant negative thermal expansion, yields a α_V of $-27.3 \text{ ppm} \cdot \text{K}^{-1}$ [64, 65]. Since SmAsFeO has a significantly larger value, it is unlikely that such a mechanism exists.

A possible alternative explanation for the detection of negative thermal expansion could be attributed to the presence of Sm. The f block elements have a rich and complex series of structural phase diagrams as a function of temperature and pressure [66–68]. The iron oxypnictides, with the addition magnetic Fe sublattice [33, 69], further complicates the effects of magneto-elastic coupling and f -electron physics in these materials. Among the rare earth compounds, crystal field induced negative thermal expansions have been noted on the order of $-2 \text{ ppm} \cdot \text{K}^{-1}$ in compounds such as TmTe [70, 71].

However, other prominent effects are noted in the vicinity of magnetic transitions, such as a coefficient of $-500 \text{ ppm} \cdot \text{K}^{-1}$ near the Curie temperature in holmium [72]. However, in the absence of features in the susceptibility, it is unlikely that this is the origin of the effect in SmAsFeO . The one example that bears the greatest similarity to SmAsFeO is the change in the electronic configuration of Sm in $\text{Sm}_{2.72}\text{C}_{60}$ [73, 74]. In this compound, a truly dramatic change in the negative thermal expansion is observed below 50 K and is believed to be due to the change in size of the Sm ion of the $4f^6d^0$ and $4f^5d^1$ electronic configurations [75] with very similar transitions seen throughout other rare-earth systems below 60 K [76–78]. The possibility of such an electronic transition in SmFeAsO can be quickly discredited by noting refinements indicate the average size increase of Sm is less than 1% and observing there exists a small but detectable negative thermal expansion below 50 K for LaFeAsO [38]. Combining the observation of $\alpha_V < 0$ for LaFeAsO and the assumption that the underlying mechanism in LaFeAsO is similar to that in SmFeAsO , provides an argument against Sm electron localisation, since the La^{3+} ions should not adopt a valence fluctuating state.

Ruling out the presence of rare-earth valence fluctuations, one can now turn to the condensation of electrons as a possible mechanism. The iron oxypnictides are itinerant electron systems with a reduced ordered iron moment consistently below $\sim 0.8 \mu_B$ within the SDW regime [1, 26, 37, 79]. The condensation of electrons from a higher occupied band to a lower band, for example, could be a possible mechanism for the negative thermal expansion, as is seen in other itinerant metals such as Cr ($-9 \text{ ppm} \cdot \text{K}^{-1}$) [75, 80], a metal that also possesses a nested Fermi surface [81]. In fact, current models of itinerant magnetism in the iron pnictides have been successful in predicting the Q -wavevector of the incommensurate ordering, and have provided an explanation for the structural phase transition as a function of doping, albeit there are key differences between various models at the present that are highly dependent on sensitive parameters [30]. Furthermore, resistivity, magnetoresistivity, Hall effect, Seebeck coefficient, infrared reflectivity measurements performed by Tropeano *et al* [39] on $\text{SmFeAsO}_{1-x}\text{F}_x$ ($x = 0$ and 0.07) alluded to a condensation of electrons from the opening of a SDW gap. In agreement with previous measurements [3, 39, 49], we note that there is a signature for the condensation of electrons in the resistivity. As shown in figure 3(d), the derivative of the resistivity exhibits a broad peak at approximately 55 K, coinciding with the onset of the negative thermal expansion and thus supporting our interpretation of the negative thermal expansion as a consequence of electronic condensation. The energy scale, on the order of T_C in optimally doped samples [19–21], suggests the possibility that the proposed electron condensation may play a key role in the mechanism of superconductivity of $\text{SmFeAsO}_{1-x}\text{F}_x$. The suppression of the negative thermal expansion down to 10 K for the fluorine-doped samples as illustrated in figures 4 and 5, suggests that the negative thermal expansion cannot be solely attributed to the superconducting phase but instead to the competing SDW phase; a phase that is also rapidly suppressed with the onset of superconductivity [1, 42, 43]. Finally, it is worthwhile to note

that μ SR measurements [82] on a variety of underdoped iron-arsenic superconductors such as $\text{LaFeAsO}_{1-x}\text{F}_x$ ($x = 0.03$) have revealed the presence of a Bessel function line shape to the relaxation, reminiscent of the behaviour of the cuprates within the ‘stripe’-ordered phase [83]. This line-shape is distinct from the parent compound LaOFeAs , and suggests that there is an electronic condensation leading to a reduced field at the muon site. Consequently, the negative thermal expansion noted in this current work may possibly be an indication of this condensation associated with ‘stripe’-like order which would be consistent with the magnetic ordering on the Sm and Fe sublattices [33].

Acknowledgments

We acknowledge useful conversations with J P Attfield, A J Browne, K H Hong, G M McNally, G Perversi, C Stock and S E Maytham. This work utilised facilities supported in part by the NSF under Agreement No. DMR-0084173. A portion of this work was made possible by the NHMFL In-House Research Program, the Schuller Program, the EIEG Program, the State of Florida, and the DOE. C R W would like to specifically acknowledge the Canada Research Chair (Tier II) program, CIFAR, NSERC, CFI and the ACS Petroleum Fund for financial support. P M S acknowledges funding from the CCSF and the University of Edinburgh through the GRS and PCDS. L B acknowledges financial support from the DOE-BES Program through Award No. DE-SC0002613.

ORCID iDs

H D Zhou  <https://orcid.org/0000-0002-1595-1912>
 P M Sarte  <https://orcid.org/0000-0002-9162-7081>
 B S Conner  <https://orcid.org/0000-0003-1738-2941>
 L Balicas  <https://orcid.org/0000-0002-5209-0293>
 C R Wiebe  <https://orcid.org/0000-0002-3681-0182>

References

- [1] de la Cruz C *et al* 2008 *Nature* **453** 12
- [2] Stewart G R 2011 *Rev. Mod. Phys.* **83** 1589
- [3] Liu R H *et al* 2008 *Phys. Rev. Lett.* **101** 087001
- [4] Stock C, Buyers W J L, Yamani Z, Tun Z, Birgeneau R J, Liang R, Bonn D and Hardy W N 2008 *Phys. Rev. B* **77** 104513
- [5] Stock C, Buyers W J L, Tun Z, Liang R, Peets D, Bonn D, Hardy W N and Taillefer L 2002 *Phys. Rev. B* **66** 024505
- [6] Stock C *et al* 2005 *Phys. Rev. B* **71** 024522
- [7] Stock C, Buyers W J L, Liang R, Peets D, Tun Z, Bonn D, Hardy W N and Birgeneau R J 2004 *Phys. Rev. B* **69** 014502
- [8] Birgeneau R J, Stock C, Tranquada J M and Yamada K 2006 *J. Phys. Soc. Japan* **75** 111003
- [9] Rodriguez E E, Stock C, Zajdel P, Krycka K L, Majkrzak C F, Zavalij P and Green M A 2011 *Phys. Rev. B* **84** 064403
- [10] Aharony A, Birgeneau R J, Coniglio A, Kastner M A and Stanley H E 1988 *Phys. Rev. Lett.* **60** 1330
- [11] Vaknin D, Sinha S K, Moncton D E, Johnston D C, Newsam J M, Safinya C R and King H E Jr 1987 *Phys. Rev. Lett.* **58** 2802
- [12] Emery V J 1987 *Phys. Rev. Lett.* **58** 2794
- [13] Bednorz J G and Müller K A 1986 *Z. Phys. B* **64** 189
- [14] Hussey N 2016 *Nat. Phys.* **12** 290
- [15] Rybicki D, Jurkatat M, Reichardt S, Kapusta C and Haase J 2016 *Nat. Commun.* **7** 11413
- [16] Lee P A, Nagaosa N and Wen X G 2006 *Rev. Mod. Phys.* **78** 17
- [17] Kamihara Y, Watanabe T, Hirano M and Hosono H 2008 *J. Am. Chem. Soc.* **130** 3296
- [18] Chen G F *et al* 2008 *Phys. Rev. Lett.* **101** 057007
- [19] Singh S J, Shimoyama J, Yamamoto A, Ogino H and Kishio K *IEEE Trans. Appl. Supercond.* **23** 7300605
- [20] Chen X H, Wu T, Wu G, Liu R H, Chen H and Fang D F 2008 *Nature* **453** 761
- [21] Zhi-An R, Wei L, Jie Y, Wei Y, Xiao-Li S, Guang-Can C, Xiao-Li D, Li-Ling S, Fang Z and Zhong-Xian Z 2008 *Chin. Phys. Lett.* **25** 2215
- [22] Rodriguez E E, Sokolov D A, Stock C, Green M A, Sobolev O, Rodriguez-Rivera J A, Cao H and Daoud-Aladine A 2013 *Phys. Rev. B* **88** 165110
- [23] Stock C, Rodriguez E E, Green M A, Zavalij P and Rodriguez-Rivera J A 2011 *Phys. Rev. B* **84** 045124
- [24] Stock C, Rodriguez E E and Green M A 2012 *Phys. Rev. B* **85** 094507
- [25] McCabe E E, Stock C, Rodriguez E E, Wills A S, Taylor J W and Evans J S O 2014 *Phys. Rev. B* **89** 100402(R)
- [26] Zhao J *et al* 2008 *Nat. Mater.* **7** 953
- [27] Wang C *et al* 2008 *Europhys. Lett.* **83** 67006
- [28] Si Q and Abrahams E 2008 *Phys. Rev. Lett.* **101** 076401
- [29] Fang C, Yao H, Tsai W F, Hu J P and Kivelson S A 2008 *Phys. Rev. B* **77** 224509
- [30] Mazin I, Singh D J, Johannes M D and Du M H 2008 *Phys. Rev. Lett.* **101** 057003
- [31] Xu C, Müller M and Sachdev S 2008 *Phys. Rev. B* **78** 020501
- [32] Mertelj T *et al* 2010 *Phys. Rev. B* **81** 224504
- [33] Nandi S *et al* 2011 *Phys. Rev. B* **84** 054419
- [34] Stock C, Buyers W J L, Yamani Z, Broholm C L, Chung J-H, Tun Z, Liang R, Bonn D, Hardy W N and Birgeneau R J 2006 *Phys. Rev. B* **73** 100504
- [35] Rodriguez E E, Stock C, Krycka K L, Majkrzak C F, Zajdel P, Kirshenbaum K, Butch N P, Saha S R, Paglione J and Green M A 2011 *Phys. Rev. B* **83** 134438
- [36] Stock C, Rodriguez E E, Sobolev O, Rodriguez-Rivera J A, Ewings R A, Taylor J W, Christianson A D and Green M A 2014 *Phys. Rev. B* **90** 121113
- [37] Kimber S A J *et al* 2008 *Phys. Rev. B* **78** 140503
- [38] Nomura T, Kim S W, Kamihara Y, Hirano M, Sushko P V, Kato K, Takata M, Shluger A L and Hosono H 2008 *Supercond. Sci. Technol.* **21** 125028
- [39] Tropeano M *et al* 2009 *Supercond. Sci. Technol.* **22** 034004
- [40] Ding L, He C, Dong J K, Wu T, Liu R H, Chen X H and Li S Y 2008 *Phys. Rev. B* **77** 180510
- [41] Margadonna S, Takabayashi Y, McDonald M T, Brunelli M, Wu G, Liu R H, Chen X H and Prassides K 2009 *Phys. Rev. B* **79** 014503
- [42] Wu J J, Lin J F, Wang X C, Liu Q Q, Zhu J L, Xiao Y M, Chow P and Jin C Q 2013 *Proc. Natl Acad. Sci. USA* **110** 17263
- [43] Dong J *et al* 2008 *Europhys. Lett.* **83** 27006
- [44] Rodríguez-Carvajal J 1993 *Physica B* **192** 55
- [45] Roisnel T and Rodríguez-Carvajal J 1999 *Mater. Sci. Forum* **378** 118
- [46] Martinelli A, Palenzona A, Ferdeghini C, Putti M and Emerich H 2009 *J. Alloys Compd.* **477** L21
- [47] Quebe P, Terbüchte L J and Jeitschko W 2000 *J. Alloys Compd.* **302** 70
- [48] Johrendt D, Hosono H, Hoffmann R-D and Pöttgen R 2011 *Z. Kristallogr. Cryst. Mater.* **226** 435
- [49] Kaciulis S, Mezzi A, Ferdeghini C, Martinelli A and Tropeano M 2010 *Surf. Interface Anal.* **42** 692

- [50] Yin Z P, Lebègue S, Han M J, Neal B P, Savrasov S Y and Pickett W E 2008 *Phys. Rev. Lett.* **101** 047001
- [51] Meena R S, Pal A, Kumar S, Rao K V R and Awana V P S 2013 *J. Supercond. Nov. Magn.* **26** 2383
- [52] Ichikawa N, Uchida S, Tranquada J M, Niemöller T, Gehring P M, Lee S H and Schneider J R 2000 *Phys. Rev. Lett.* **85** 1738
- [53] Klauss H H et al 2008 *Phys. Rev. Lett.* **101** 077005
- [54] McGuire M A et al 2008 *Phys. Rev. B* **78** 094517
- [55] Rotter M, Tegel M, Schellenberg I, Schappacher F M, Pöttgen R, Deisenhofer J, Günther A, Schrettle F, Loidl A and Johrendt D 2009 *New J. Phys.* **11** 025014
- [56] Klingeler R, Wang L, Köhler U, Behr G, Hess C and Büchner B 2010 *J. Phys.: Conf. Ser.* **200** 012088
- [57] Klimczuk T et al 2012 *Phys. Rev. B* **85** 174506
- [58] Chen J, Hu L, Deng J and Xing X 2015 *Chem. Soc. Rev.* **44** 3522
- [59] White M A, Lushington K J and Morrison J A 1978 *J. Chem. Phys.* **69** 4227
- [60] Barrera G D, Bruno J A O, Barron T H K and Allan N L 2005 *J. Phys.: Condens. Matter* **17** R217
- [61] Lightfoot P, Woodcock D A, Maple M J, Villaescusa L A and Wright P A 2001 *J. Mater. Chem.* **11** 212
- [62] Scheel K 1907 *Verh. Dtsch. Phys. Ges.* **9** 718
- [63] Attfield M P, Feyngenson M, Neuefeind J C, Proffen T E, Lucas T C A and Hriljac J A 2016 *RSC Adv.* **6** 19903
- [64] Mary T A, Evans J S O, Vogt T and Sleight A W 1996 *Science* **272** 90
- [65] Sleight A W 1998 *Annu. Rev. Mater. Sci.* **28** 29
- [66] Taylor K N R and Darby M I 1972 *Physics of Rare Earth Solids* (London: Chapman and Hall)
- [67] Savrasov S Y, Kotliar G and Abrahams E 2001 *Nature* **410** 793
- [68] Söderlind P, Nordström L, Yongming L and Johansson B 1990 *Phys. Rev. B* **42** 4544
- [69] Ryan D H, Cadogan J M, Ritter C, Canepa F, Palenzona A and Putti M 2009 *Phys. Rev. B* **80** 220503
- [70] Ott H R and Lüthi B 1977 *Z. Phys. B* **28** 141
- [71] Bergmann H 2013 Sc, Y, La–Lu rare earth elements: compounds with Te, Po *Gmelin Handbook of Inorganic and Organometallic Chemistry* 8th edn (Berlin: Springer)
- [72] White G K 1989 *J. Phys.: Condens. Matter* **1** 6987
- [73] Brown S, Cao J, Musfeldt J L, Drago N, Cimpoesu F, Ito S, Takagi H and Cross R J 2006 *Phys. Rev. B* **73** 1254
- [74] Arvanitidis J, Papagelis K, Margadonna S, Prassides K and Fitch A N 2003 *Nature* **425** 599
- [75] Grima J N, Oliveri L, Ellul B, Gatt R, Attard D, Cicala G and Recca G 2010 *Phys. Status Solidi—RRL* **4** 133
- [76] Mattens W C M, Hölscher H, Tuin G J M, Moleman A C and de Boer F R 1980 *J. Magn. Magn. Mater.* **15** 982
- [77] Mook H A, McWhan D B and Holtzberg F 1982 *Phys. Rev. B* **25** 4321(R)
- [78] Kuznetsov A Y, Dmitriev V P, Bandilet O I and Weber H P 2003 *Phys. Rev. B* **68** 064109
- [79] Chen Y, Lynn J W, Li J, Li G, Chen G F, Luo J L, Wang N L, Dai P C, de la Cruz C and Mook H A 2008 *Phys. Rev. B* **78** 064515
- [80] Takenaka K 2012 *Sci. Tech. Adv. Mater.* **13** 013001
- [81] Fawcett E 1988 *Rev. Mod. Phys.* **60** 209
- [82] Carlo J P et al 2009 *Phys. Rev. Lett.* **102** 087001
- [83] Savici A T et al 2002 *Phys. Rev. B* **66** 014524